Wang, Xiyu; Duan, Ruifeng; Yigitler, Yusein; Menta, Estifanos; Jäntti, Riku

Machine Learning-Assisted Detection for BPSK-modulated Ambient Backscatter Communication Systems

Published in:
IEEE Global Communications Conference

DOI:
10.1109/GLOBECOM38437.2019.9013284

Published: 01/01/2019

Document Version
Peer reviewed version

Machine Learning-Assisted Detection for BPSK-modulated Ambient Backscatter Communication Systems

Xiyu Wang, Ruifeng Duan, Hüseyin Yiğitler, Estifanos Yohannes Menta, and Riku Jäntti
Department of Communications and Networking, Aalto University, Espoo, 02150 Finland.
e-mail: {xiyu.wang; ruifeng.duan; yusein.ali; estifanos.menta; riku.jantti}@aalto.fi

***Abstract*—Ambient backscatter communication (AmBC), a green communication technology, is hampered by the continuously and extremely fast varying, strong and unknown ambient radio frequency (RF) signals. This paper presents a machine learning-assisted method for extracting the information of the AmBC device. The information is modulated on top of the unknown Gaussian-distributed ambient RF signals. The proposed approach can decode the binary phase shift keying backscatter signals encoded using Hadamard codes. This method extracts the learnable features for the tag signal by first eliminating the direct path signal and then correlating the residual signal with the coarse estimate of ambient signal. Thereafter, the tag signals are recovered by using the k-nearest neighbors classification algorithm. The recovered signals are decoded by a Hadamard decoder to retrieve the original information bits. We validate the performance using simulations to corroborate the proposed approach.**

***Index Terms*—Ambient backscatter, classification algorithm, green communication, machine learning, signal detection.**

I. Introduction

The generation of wireless communications is innovating with the advent of ubiquitous data transmission era that information are acquired and conveyed among devices, which is known as Internet-of-Things (IoT) [1]. The extensive connections and massive deployment of IoT sensors incur two main challenges naturally in wireless communication systems, namely the scarcity spectrum resource and power consumption. With this regard, ambient backscatter communication (AmBC) scheme stands out [2], since the tags do not have power-hungry amplifiers and do not need to generate own carrier signals. This technology has been considered one of 10 breakthrough technologies in green wireless communications by MIT Technology Review [3]. In AmBC systems, a passive tag senses and gathers information in the environment, and delivers these collected data by directly modulating on top of the ambient radio frequency (RF) signals, such as cellular network [4], WiFi [5], and digital video broadcasting - terrestrial (DVB-T) [6]. Hence, significant bandwidth efficiency enhancement can be obtained owing to the spectrum share of the AmBC system and the legacy system [7]. Possessing the aforementioned properties, AmBC technology is prone to become an important component of future sustainable IoT ecosystems.

To retrieve the information of the AmBC system, typical detectors, for instance, maximum likelihood and energy detectors have been investigated in literature for on-off-keying (OOK) based backscatter systems [8]–[10]. Authors in [8] have tackled the problems of detecting PSK-modulated tag signals by a maximum likelihood detector, where the corresponding decision regions have been obtained. In orthogonal frequency-division multiplexing (OFDM) systems, the presence of tag signals introduces frequency shift to the ambient signals. Hence, tag signals can be extracted by exploiting the cyclic prefix part [9] or guard bands between OFDM symbols [10]. However, energy detection usually introduces an error floor in high signal-to-noise ratio (SNR) regime [11] and requires high spreading gain to measure the power level. Also, the bit rate of the AmBC system is on the same or lower order of the OFDM symbol rate of the legacy system.

Meanwhile, the pervasive information interaction within large amount of devices will drive an exponential growth in wireless data traffic. The requirements of real-time and rapid processing of large volume data have been leading rise of implementing machine learning (ML) techniques to wireless communications [12]. Applying ML techniques to AmBC receiver designs has attracted much attention recently, such as regression analysis as means to estimate channels [13] and signal inference through exploring the patterns of received signal belonging to different classes [5], [14]. A decoder in [5] is proposed based on a unique slope pattern generated from smoothing of receiving WiFi signals by feature extraction process [15]. In [13], the authors have proposed a blind channel estimation scheme using the expectation maximization (EM) algorithm for an OOK-modulated backscattering system. Two EM-based constellation learning algorithms are proposed in [14] in both labeled and unlabeled contexts with the knowledge of the constellation set of the ambient RF signals.

Another challenging issue for the AmBC systems is that the direct path is orders of magnitude stronger than that of the backscattered path, since there are two (composite) paths of signals impinging to the AmBC receiver. This strong signal component of the legacy system drastically degrades the signal-to-interference-plus-noise ratio (SINR) of the AmBC signal[1]. Several methods have been proposed in literature to

[1]In this work, we assume that the legacy and AmBC systems share the same frequency bands.

handle this issue, for instance, [4], [14], [16]–[18]. Authors in [4] have used two receive antennas to mitigate the unknown direct path. In the theoretical analysis, the legacy signals are jointly decoded assuming that channel coefficients are available at the receiver [16]. The work [18] has designed a hybrid beamforming method to separate two paths in a multi-antenna scenario, which acquires spreading gain by using Hadamard codes [18]. Relying on the knowledge of the constellation set of the ambient RF signals at the AmBC receiver, [14] has applied EM-assisted methods to retrieve the OOK-modulated backscatter information.

Nevertheless, the requirement of the finite number of the ambient RF signal constellations known at the receiver hampers the detection performance. The considerably high-order constellation sets practically exist, for instance, in DVB-T and WiFi systems. In addition, since a legacy system has much higher data transmission rate than an AmBC system, the phase of the legacy system symbol varies rapidly from one to another resulting in very fast fading seen by the AmBC link.

To address the above challenges, we propose an ML-assisted AmBC detector design that extracts learnable features by first treating backscattered path as interference and projecting the received signal to the orthogonal space of the direct path signal. Following the direct path interference elimination, the residual signal is augmenting in the signal space and correlating with the coarse estimate of ambient signal. We can apply ML classification algorithms towards the processed data to detect the tag signal. The following summarizes the main contributions of the proposed general ML-assisted method for AmBC systems which can operate with reasonable performance in terms of the bit error rate (BER).

- The proposed design does not require the knowledge of the ambient RF signal constellations, and the size of the constellations can be very large, for instance, going to be infinite.
- The AmBC device applies binary phase shift keying (BPSK) modulation in order to obtain higher spectral efficiency than OOK scheme.

The rest of the paper is organized as follows. The system model is outlined in Section II. In Section III, we present our proposed method, and Section IV shows the simulation results of our proposed method. Finally, Section V concludes the paper.

II. System Model

Consider a typical bi-static AmBC system model illustrated in Fig. 1. It consists of a legacy ambient source (Tx), a single-antenna backscatter device (Tag) and an M-antenna receiver (Rx). The M antennas form a linear array with antenna spacing α. We consider that there are dominant paths between the Tx and the Rx, between the TX and the Tag, and between the Tag and the Rx. The key-hole property of the backscattered path drastically reduces the SNR of the tag signal at the Rx.

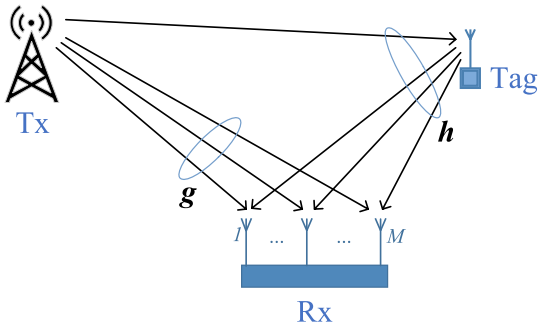

Fig. 1. An illustration of the AmBC systems.

Adopting a well-known path loss model, we represent the path losses of the direct path and the backscattered path as

$$g = \frac{\lambda^2}{(4\pi d_0)^2}, \quad h = \frac{\lambda^2}{(4\pi d_1)^2(4\pi d_2)^2},$$

where $d_i, i \in \{0, 1, 2\}$ denotes the distances of Tx-Rx, Tag-Rx and Tx-Tag, respectively, and λ is the carrier wavelength. Without loss of generality, we define $\Delta = 10\log_{10}(g/h)$ as the power difference between the direct path and the backscattered path.

Denote φ_g and φ_h as the angle of arrival (AoA) of dominant components of the direct path and the backscatter path, respectively. The directional cosines with respect to the receive antenna array are $\Omega_i = 2\pi\alpha\cos\varphi_i/\lambda, \forall i \in \{g, h\}$. The unit spatial signatures at Rx antennas read

$$\mathbf{a}_i = \frac{1}{\sqrt{M}}[1 \;\; \exp\{j\Omega_i\} \;\; \cdots \;\; \exp\{j(M-1)\Omega_i\}]^H, \forall i \in \{g, h\}. \tag{1}$$

Then the direct channel vector and the backscattered channel vector are ready to be given as $\mathbf{g} = g\mathbf{a}_g$ and $\mathbf{h} = h\mathbf{a}_h$, respectively.

We consider the AmBC tag adopting BPSK modulation scheme, i.e., the information symbol $x \in \{-1, +1\}$. The AmBC device consists of a Hadamard encoder to encode the backscatter information bits. A length-$n = 2^r$ Hadamard codeword with order of r is obtained from a Hadamard matrix of $n \times n$ over $\{+1, -1\}$. We consider systematic encoding that a length-n codeword has $r+1$ information bits with positions indexes of $\{0, 2^0, 2^1, \cdots, 2^{r-1}\}$. Hence, maximum $2^{r-2} - 1$ errors of each codeword can be corrected. The Hadamard code generator G_r with order r can be expressed as [19]:

$$G_r = \begin{bmatrix} G_{r-1} & J_{r-1} \oplus G_{r-1} \\ 0 \;\; 0 \cdots \;\; 0, & 1 \;\; 1 \cdots \;\; 1 \end{bmatrix}, \quad r \geq 3, \tag{2}$$

where J_{r-1} and G_{r-1} have the same size, $\oplus$ is the binary addition operator, and

$$G_2 = \begin{bmatrix} 1 & 0 & 0 & 1 \\ 0 & 1 & 0 & 1 \\ 0 & 0 & 1 & 1 \end{bmatrix}, \quad J_r = \begin{bmatrix} 1 & 1 & \cdots & 1 \\ 0 & 0 & \cdots & 0 \\ \vdots & \vdots & \ddots & \vdots \\ 0 & 0 & \cdots & 0 \end{bmatrix}.$$

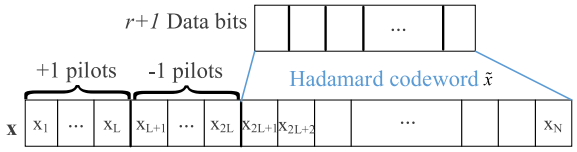

Fig. 2. The frame structure of tag signals over one CCT.

Define $\boldsymbol{b}_r = \begin{bmatrix} b(0) & b(1) & \cdots & b(r) \end{bmatrix}$ as the information bits sequence of the AmBC system. The corresponding Hadamard codeword can be obtained from $\boldsymbol{b}_r$ as following

$$\tilde{\boldsymbol{x}} = \boldsymbol{b}_r G_r. \tag{3}$$

We take one channel coherent time (CCT) into consideration[2], during which the channels are staying constant. Fig. 2 describes the frame structure of tag signals. An original sequence storing the tag information first is grouped into $(r+1)$-bit segments and then encoded into a length-n Hadamard codeword using (3). To form a frame, two length-L pilot sequences are prefixed to a codeword, which are associated to $+1$ and -1 and are known at the Rx. Without loss of generality, the total pilot sequence is set as $x_1 = \cdots = x_L = +1, x_{L+1} = \cdots = x_{2L} = -1$. Hence, the frame length N becomes $2L+n$, where $n = 2^r$, i.e., $N = 2L + 2^r$. A frame of the AmBC tag signal can be represented as $\mathbf{x} = \begin{bmatrix} x_1 & \cdots & x_L & x_{L+1} & \cdots & x_{2L} & \tilde{\boldsymbol{x}} \end{bmatrix}$.

Assume that the tag and the ambient source adopt the same data rate, and one CCT contains N samples. Denote $\mathbf{s} = [s_1 \cdots s_N]$ the ambient signal sample sequence, and $s_i \sim \mathcal{CN}(0,1), \forall i \in [1, N]$. This is a practical assumption for OFDM systems [20]. We assume the ambient source signals are i.i.d over different samples. We consider that the ambient signal $\mathbf{s}$ is unknown at the AmBC receiver. In addition, the exact channel state information is not available at the AmBC receiver. Consequently, the received signal of the i-th sample $\mathbf{y}_i \in \mathbb{C}^{M\times 1}, i = 1, \cdots, N$ reads

$$\begin{aligned} \mathbf{y}_i &= \sqrt{\text{snr}}\,(\mathbf{g}s_i + \mathbf{h}s_i x_i) + \boldsymbol{\omega_i} \\ &= \sqrt{\text{snr}}\left[g\mathbf{a}_g s_i + h\mathbf{a}_h(s_i x_i)\right] + \boldsymbol{\omega_i}, \end{aligned} \tag{4}$$

where snr is the SNR of direct path, and $\boldsymbol{\omega_i}$ denotes the additive white Gaussian noise which is assumed to be uncorrelated at the receiver antenna elements, i.e., $\boldsymbol{\omega_i} \in \mathcal{CN}(0, \mathbf{I})$.

III. Detection Design

The four-step detection design is presented in this section. Fig. 3 illustrates the workflow of the detection design. The strong direct path signal is eliminated through projecting the received signal into its orthogonal space. The second step is to augment the residual signal in the signal space and to remove partial influence of ambient signal. An ML classification algorithm is applied to classify the transmitted encoded bits of the tag, followed by the decoding of desired bits.

[2]We assume that the CCT is the same as one AmBC tag frame which is equal to the total length of the training pilots and one codeword.

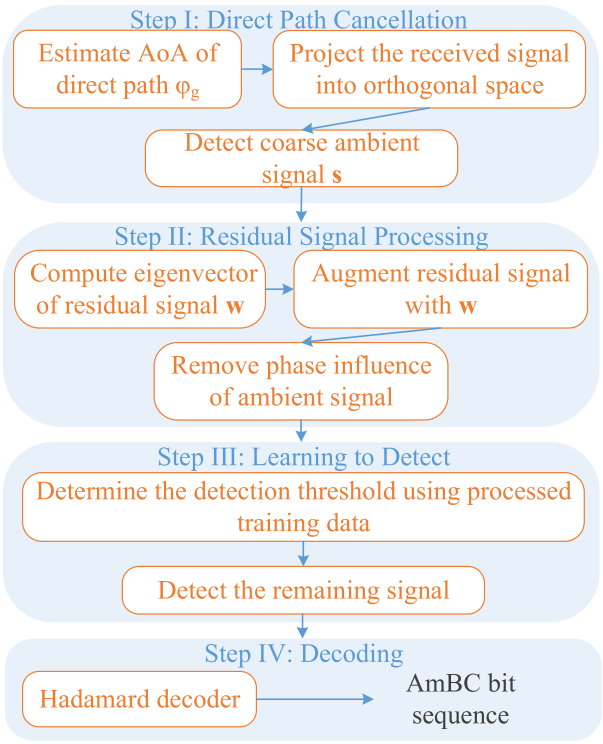

Fig. 3. Flowchart of the proposed ML-assisted tag signal detection scheme.

A. Direct path interference elimination

This subsection discusses the procedure of eliminating the strong direct path interference. To effectively extract the tag signal, the strong direct path interference needs to be eliminated beforehand in order to increase the SINR of the backscattered ambient signal. We apply a conventional Bartlett beamforming to estimate the AoA of backscattered path, φ_g. Bartlett searches a direction that magnifies the output power [21], which can be written as

$$\hat{\varphi}_g = \max_{\varphi_g} \frac{\mathbf{a}_g^H \mathbf{R} \mathbf{a}_g}{\mathbf{a}_g^H \mathbf{a}_g}, \tag{5}$$

where $\mathbf{R}$ denotes the sample covariance matrix of the received signal. With the estimated AoA $\hat{\varphi}_g$, the unit spatial signature is ready to be given based on (1) expressed as $\hat{\mathbf{a}}_g$, and $||\hat{\mathbf{a}}_g||^2 = 1$. Then we eliminate the direct path interference by projecting the received signal into an orthogonal space, which gives the residual signal

$$\mathbf{r}_i = \left(\mathbf{I} - \frac{\hat{\mathbf{a}}_g \hat{\mathbf{a}}_g^H}{||\hat{\mathbf{a}}_g||^2}\right)\mathbf{y}_i = \left(\mathbf{I} - \hat{\mathbf{a}}_g \hat{\mathbf{a}}_g^H\right)\left[\sqrt{\text{snr}} h \mathbf{a}_h(s_i x_i) + \tilde{\omega}\right], \tag{6}$$

where $\tilde{\omega}$ includes the remaining direct path interference as well as the projected Gaussian noise. The coarse estimate of ambient signal is given by

$$\hat{s}_i = \hat{\mathbf{a}}_g^H \mathbf{y}_i. \tag{7}$$

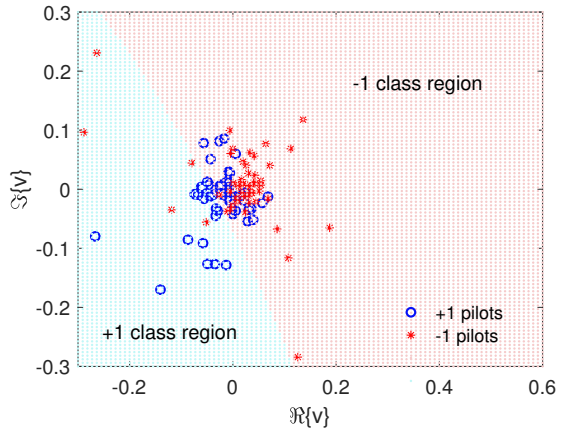

Fig. 4. Visualization of the processed training samples given SNR = 28 dB, $L = 50$ and $d_1 = 3$ meters. The decision regions are marked while adopting the SVM algorithm with RBF kernel.

Algorithm 1 kNN for obtaining distorted codewords

Input: $\mathbf{v}$, L, and k
labels$(1 : L) = +1$, labels$(L + 1 : 2L) = -1$
for $i = 2L + 1$ to N **do**
  for $j = 1$ to $2L$ **do**
    dist(i,j) $= |v_j - v_i|^2$
  end for
  Find k neatest neighbors: Nk $= \min_j$ dist(i,j)
  $\hat{w}(i - 2L) \leftarrow$ most votes from labels(Nk)
end for
Output: $\hat{w}$

B. Process of Residual signal

Given the residual signal expressed as (6), we calculate the equivalent beamformer

$$\mathbf{w} = \left(\mathbf{I} - \hat{\mathbf{a}}_g \hat{\mathbf{a}}_g^H\right) \mathbf{a}_h, \tag{8}$$

which coincides with the largest eigenvector of sample covariance matrix of residual signal. Then performing beamforming yields

$$u_i = \mathbf{w}^H \mathbf{r}_i. \tag{9}$$

Since the ambient signal has been estimated during the first step, we can roughly eliminate the phase uncertainty of the ambient signal by

$$v_i = (\hat{s}_i^H u_i)/||\hat{s}_i||^2 = \frac{\mathbf{y}_i^H \hat{\mathbf{a}}_g \mathbf{a}_h^H \left(\mathbf{I} - \hat{\mathbf{a}}_g \hat{\mathbf{a}}_g^H\right) \mathbf{y}_i}{||\hat{s}_i||^2} \tag{10}$$

C. Learning to Detect

In the previous section, the channel estimates and the ambient signal can be generally inaccurate. This section introduces an ML classification algorithm to cluster the received tag signal samples.

As the processed signal $\mathbf{v} = [v_1, \cdots, v_N]$ is a complex vector, we treat the real and the imaginary part of $\mathbf{v}$, i.e., $(\Re\{\mathbf{v}\}, \Im\{\mathbf{v}\})$, as two features. Fig. 4 visualizes two length-50 pilot sequences, each of which is associated to a class label +1 or -1, respectively[3]. In the feature space, the processed signal $\mathbf{v}$ falls into two clusters. This encourages us to apply classification algorithms for tag signal extraction. These two length-L pilot sequences are utilized as training sets to decide the threshold for differentiating two clusters and further decoding the desired information bits.

Remark: There are several candidates for classifiers, such as linear classifier, support vector machine (SVM) and k-nearest neighbors (kNN). Considering the AmBC systems, there exist outliers especially for the low-SINR situation of the backscattered signal so that the linear classifiers are not suitable in our design. Moreover, a short pilot sequence should be designed in order to improve the throughput of the Tag. However, a short training set produces uncertain decision hyperplanes of SVM. And SVM becomes unstable because the support vectors can be significantly affected by the outliers. In Fig. 4, we also depict the decision regions of two classes while applying the SVM algorithm with the radial basis function (RBF) kernel. It can be readily observed that the non-linear SVM generates inaccurate classifications of tag signal. Hence, we apply kNN algorithm for classification.

Specifically, all $2L$ training examples are stored. In order to classify a new unlabeled sample, distances between this new sample and $2L$ training sets are calculated. The new data is assigned to the class which owns plurality votes among k selected nearest neighbors. The major process of kNN is presented in Algorithm 1 where $\hat{w}$ denotes the distorted received codeword over $\{+1, -1\}$ obtained after classification. Note that there is a tradeoff between the number k and the performance of the kNN method. The selection of k is dataset-dependent. A higher value of k has less chance of error. However, it leads to unclear decision boundaries.

D. Hadamard decoder

After obtaining the distorted codewords $\hat{w}$, a Hadamard decoder [19] is applied to retrieve the original AmBC information bits. We calculate $\tilde{w} = \hat{w}\mathcal{H}_n$, where $\mathcal{H}_n$ denotes an $n \times n$ Hadamard matrix, $n = 2^r$, r is the codeword order, and $2^{r-2}-1$ errors of each codeword can be corrected. We consider $r \geq 3$ in this paper. Define t be the index of the maximum value of $|\tilde{w}|$. The corrected codeword reads

$$\hat{x} = \begin{cases} 2(\mathsf{mod}(2\mathcal{H}(1,:) - \mathcal{H}(t,:), 3)) - 1, & \text{for } \tilde{w}(t) \geq 0 \\ 2(\mathsf{mod}(2\mathcal{H}(1,:) + \mathcal{H}(t,:), 3)) - 1, & \text{for } \tilde{w}(t) < 0, \end{cases}$$

where mod denotes the Modulus operator. The decoded information sequence can be retrieved from $\hat{x}$ by selecting the information bits with positions indexes of $\{0, 1, 2, \cdots, 2^{r-1}\}$. Finally, after retrieving all the transmitted information bits, the bit error rate of the AmBC system can be readily obtained.

[3]This figure is taken from one CCT. Note that positions of the clusters vary with channel conditions and the SNR of legacy system.

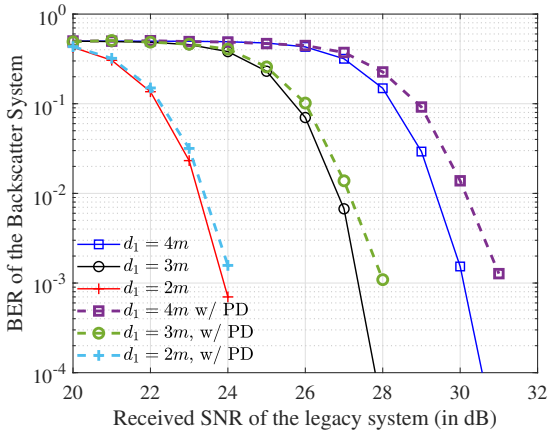

Fig. 5. AmBC BER as a function of the SNR of the legacy system (direct path) using kNN learning algorithm. The Hadamard codeword has a length of $n = 2^{10}$. The size of training dataset $L = n$. The solid/dashed lines show the scenarios without/with considering phase distortion at the receiver, respectively.

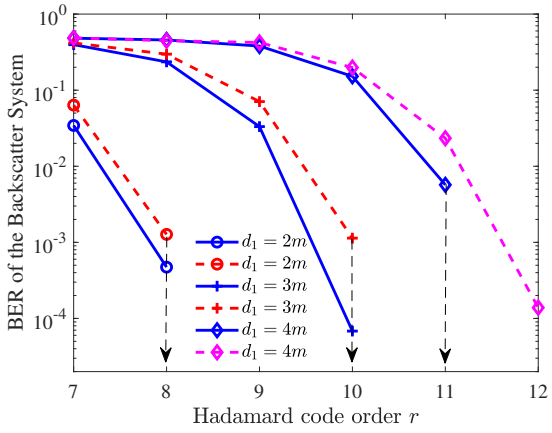

Fig. 6. AmBC BER as a function of the Hadamard code order $r = \log_2 n$ which is an integer. The size of training dataset $L = n$. The received SNR of the legacy system (direct path) is set to 28dB.

IV. Numerical Results

In this section, simulation results are provided to validate the performance of the proposed detection method. We consider a practical scenario that the carrier frequency of ambient RF source is 500 MHz and the required minimum SNR is approximately 20 dB at the cell edge, for instance, DVB-T systems. Recall that the power of the direct path is orders of magnitude stronger than that of the backscattered path. We set the distance between the Tx and the Rx d_0 being 1000 meters and the distance between the backscatter and the Rx d_1 being $2, 3$, and Process the Residual signal 4 meters. The relevant power differences between two paths are illustrated in Table I. We consider that the linear receive antenna array has $M = 8$ elements with half-wavelength antenna separation, i.e., $\alpha = \lambda/2$. The Tx is located at the direction of 82°, while the Tag is at 120°(The directions affect the results when using linear antenna array). We consider that the Tag adopts BPSK modulation scheme and has no channel state information. We choose $k = 5$ closest neighbors for the kNN algorithm. The standard variance of the phase distortion at the receiver, for instance, caused by the ADC converter, σ, is set to 0.03491 in radians. All results are obtained by averaging over 10^5 Monte Carlo realizations (AmBC frames).

TABLE I
Power difference between two paths with d_1

d_1 (meter)	2	3	4
Δ(dB)	32.4	35.9	38.4

Fig. 5 depicts the BER of the proposed design as a function of the direct path SNR. The size of training set (associated to one backscatter symbol, i.e., $+1$ or -1) is equal to the length of codeword, i.e., $L = n = 2^r = 1024$. The solid curves show that there is no phase distortion (PD) at the receiver, while the dashed ones represent the practical scenarios with phase distortion. It is clear that a small distance increment between the backscatter and the receiver results in huge performance loss. In addition, the proposed approach eliminates the error floor issue existing in traditional energy detection (for amplitude modulation schemes) in high SNR region, for instance, as the SNR of the direct path exceeds approximately 24 dB and $d_1 = 2$ meters, all backscatter information bits can be retrieved without error (we transmitted 11×10^5 bits, i.e, number of realizations $\times(r + 1)$, and did not detect an error.).

Fig. 6 illustrates the BER as a function of Hadamard code order r provided the SNR of the direct path at the receiver being 28 dB. The size of training set of one backscatter symbol is equal to the length of codeword, i.e., $L = n = 2^r$. It is clearly shows that using longer codeword is required to improve the BER. In Fig.7, we show the BER as a function of the length of a training sequence L, which is an integer. The Hadamard code order is set to $r = 10$. The received SNR of the legacy system (direct path) is set to 28dB. Observed from the curves, increasing the training set length also can improve the BER, since a longer training set provides more samples for the classifier.

V. Conclusion

In this paper, we proposed a detection method of the tag signal based on ML techniques, using classification algorithm, kNN. Considering the legacy system operating with normal SNR regime, the design enables the AmBC system to retrieves the BPSK-modulated information with practically acceptable performance without having the knowledge of the channel information and the constellations of the legacy system. This promotes the applications of AmBC in practice. Although this method was assumed based on a simple system model, it can be extended to more complex settings, such as higher order modulation schemes and multiple-tag scenarios, which are our future research direction.

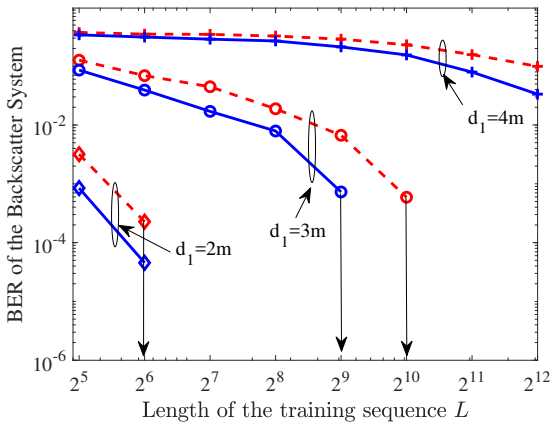

Fig. 7. AmBC BER as a function of the length of a training sequence L, which is an integer. The Hadamard code order is set to $r = 10$. The received SNR of the legacy system (direct path) is set to 28dB.

ACKNOWLEDGMENT

This work was supported in part by the Academy of Finland under Project No. 311760 and Project No. 319003, and the China Scholarship Council (CSC).

REFERENCES

[1] M. R. Palattella, M. Dohler, A. Grieco, G. Rizzo, J. Torsner, T. Engel, and L. Ladid, "Internet of Things in the 5G era: Enablers, architecture, and business models," *IEEE J. Sel. Areas Commun.*, vol. 34, no. 3, pp. 510–527, Mar. 2016.

[2] V. Liu, A. Parks, V. Talla, S. Gollakota, D. Wetherall, and J. R. Smith, "Ambient backscatter: Wireless communication out of thin air," in *Proc. ACM SIGCOMM'13*, Hong Kong, China, Aug. 2013, pp. 39–50.

[3] M. Harris, "10 breakthrough technologies 2016: Power from the air," online, Feb. 2016. [Online]. Available: https://www.technologyreview.com/s/600773/10-breakthrough-technologies-2016-power-from-the-air/

[4] A. N. Parks, A. Liu, S. Gollakota, and J. R. Smith, "Turbocharging ambient backscatter communication," in *Proc. ACM SIGCOMM'14*, Chicago, IL, Aug. 2014, pp. 619–630.

[5] H. Hwang, J. H. Lim, J. Yun, and B. J. Jeong, "Pattern-based decoding for Wi-Fi backscatter communication of passive sensors," *Sensors*, vol. 19, no. 5, Feb. 2019.

[6] R. J. Vyas, B. B. Cook, Y. Kawahara, and M. M. Tentzeris, "E-WEHP: A batteryless embedded sensor-platform wirelessly powered from ambient digital-TV signals," *IEEE Trans Microw Theory Tech.*, vol. 61, no. 6, pp. 2491–2505, Jun. 2013.

[7] R. Duan, R. Jäntti, H. Yiğitler, and K. Ruttik, "On the achievable rate of bistatic modulated rescatter systems," *IEEE Trans. Veh. Technol.*, vol. 66, no. 10, pp. 9609–9613, Oct. 2017.

[8] J. Qian, A. N. Parks, J. R. Smith, F. Gao, and S. Jin, "IoT communications with m-PSK modulated ambient backscatter: Algorithm, analysis, and implementation," *IEEE Internet Things J.*, vol. 6, no. 1, pp. 844–855, Feb. 2019.

[9] G. Yang, Y.-C. Liang, R. Zhang, and Y. Pei, "Modulation in the air: backscatter communication over ambient OFDM carrier," *IEEE Trans. Commun.*, vol. 66, no. 3, pp. 1219–1233, Mar. 2018.

[10] M. A. ElMossallamy, M. Pan, R. Jäntti, K. Seddik, G. Li, and Z. Han, "Noncoherent backscatter communications over ambient OFDM signals," *IEEE Trans. Commun.*, 2019, in print.

[11] Z. Ma, T. Zeng, G. Wang, and F. Gao, "Signal detection for ambient backscatter system with multiple receiving antennas," in *Proc. IEEE Canadian Workshop Inf. Theory*, St. John's, NL, Canada, Jul. 2015, pp. 50–53.

[12] C. Jiang, H. Zhang, Y. Ren, Z. Han, K. Chen, and L. Hanzo, "Machine learning paradigms for next-generation wireless networks," *IEEE Wireless Communications*, vol. 24, no. 2, pp. 98–105, April 2017.

[13] S. Ma, G. Wang, R. Fan, and C. Tellambura, "Blind channel estimation for ambient backscatter communication systems," *IEEE Commun. Lett.*, vol. 22, no. 6, pp. 1296–1299, Jun. 2018.

[14] Q. Zhang, H. Gao, Y. Liang, and X. Yuan, "Constellation learning lased signal detection for ambient backscatter communication systems," *IEEE J. Sel. Areas. Commun.*, vol. 37, no. 2, pp. 452–463, Feb. 2019.

[15] I. Guyon and A. Elisseeff, *An Introduction to Feature Extraction*. Berlin, Heidelberg: Springer Berlin Heidelberg, 2006, pp. 1–25.

[16] G. Yang, Q. Zhang, and Y. Liang, "Cooperative ambient backscatter communications for green Internet-of-Things," *IEEE Internet Things J.*, vol. 5, no. 2, pp. 1116–1130, Apr. 2018.

[17] R. Duan, R. Jäntti, M. A. ElMossallamy, Z. Han, and M. Pan, "Multi-antenna receiver for ambient backscatter communication systems," in *Proc. IEEE SPAWC*, Kalamata, Greece, Jun. 2018.

[18] R. Duan, E. Y. Menta, H. Yigitler, R. Jäntti, and Z. Han, "Hybrid beamformer design for high dynamic range ambient backscatter receivers," *CoRR*, 2019. [Online]. Available: http://arxiv.org/abs/1901.05323

[19] G. Yue, L. Ping, and X. Wang, "Generalized low-density parity-check codes based on Hadamard constraints," *IEEE Trans. Inf. Theory*, vol. 53, no. 3, pp. 1058–1079, Mar. 2007.

[20] S. Wei, D. L. Goeckel, and P. A. Kelly, "Convergence of the complex envelope of bandlimited OFDM signals," *IEEE Trans. Inf. Theory*, vol. 56, no. 10, pp. 4893–4904, Oct. 2010.

[21] H. Krim and M. Viberg, "Two decades of array signal processing research: the parametric approach," *IEEE Signal Process. Mag.*, vol. 13, no. 4, pp. 67–94, Jul. 1996.